International Journal of Mechanical, Industrial and Aerospace Sciences
ISSN: 2517-9950
Vol:8, No:5, 2014

Large Eddy Simulation of Flow Separation Control over a NACA2415 Airfoil

M. Tahar Bouzaher

***Abstract*—**This study involves a numerical simulation of the flow around a NACA2415 airfoil, with a 15°angle of attack, and flow separation control using a rod, It reposes inputting a cylindrical rod upstream of the leading edge in order to accelerate the transition of the boundary layer by interaction between the rod wake and the boundary layer. The viscous, non-stationary flow is simulated using ANSYS FLUENT 13. Our results showed a substantial modification in the flow behavior and a maximum drag reduction of 51%.

***Keywords*—**CFD, Flow separation, Active control, Boundary layer, rod, NACA 2415.

I. Introduction

THE need to understand low Reynolds number aerodynamics has gained more attention due to variety of mechanical applications like Unmanned Air Vehicle (UAV), Micro Air Vehicle (MAV) and wind turbine.[1] The presence of laminar separation bubble has a deteriorating effect on the performance of these vehicle. The understanding of the physics of this bubble and the possible ways of control become an essential prerequisite for an efficient design of these systems. M. Serdar Genç et al. [1] studied the boundary layer separation on a NACA2415 airfoil using hot-wire anemometry and oil flow visualization method, to photograph the surface flow patterns. The experimental results showed that when the angle of attack increases, the separation and the transition points move towards the leading edge. Mittal et al. [2] characterized the different frequencies scales present in a separated flow to understand the physical of the separation control by steady and pulsed vortex Generator Jets. The review of Greenblatt et al. [3] summarized the flow separation control by periodic excitation in various forms. Flow control through boundary layer can reduce the drag, enhance the lift, and improve the performance of aircraft. Among the used methods, vortex generators (VG) have been widely used. Igarashi et al. [4] use a rod as vortex generators to control the flow around a square cylinder for a Reynolds number of 3.2×10^4, the results shows a drag reduction of 50% with taking into account the drag of the cylindrical rod. For a Reynolds number located in the range $1.9 \times 10^4 \leq Re \leq 7.7 \times 10^4$.The experimental study of Igarashi et al. [5] on the effect of the interaction between the wake of a cylindrical rod, and the boundary layer of a vertical disc has proved that it is possible to reduce the drag of 20 to 30% compared to natural case (in the absence of the cylindrical rod). Tsutsui et al [6] set the cylindrical rod to a circular cylinder in order to reduce drag force; they have found that the optimal conditions for a maximum drag reduction (63%) are $d / D = 0.25$. The aim of this work is to study the flow separation control using a rod-airfoil configuration. The study focuses on estimating of the characteristic aerodynamics and the efficiency of this strategy in drag reduction.

M. T. Bouzaher is a Research Associate at the Department of Mechanical Engineering of the University of Biskra,07000, Algeria (e-mail: mohamedbouzaher@yahoo.fr).

II. Geometry Characteristics and Mesh Generation

We considered five positions of the cylindrical rod. The choice of the positions is based on the mode of the flow (shedding vortices) around the rod.

Owing the reason that a quadrilateral grid captures the boundary layer more precisely than a triangular grid. We used a quadrilateral grid and we divided the calculation domain into two zones (Fig. 2). This allows keeping the same mesh in the close area surrounding the Rod-foil.

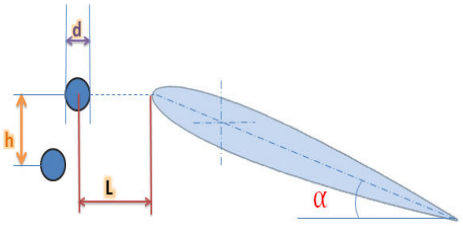

Fig. 1 Rod-foil geometrical characteristics

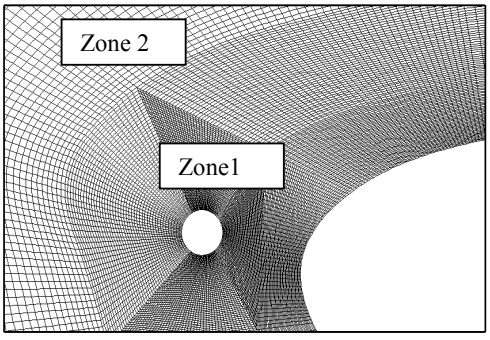

Fig. 2 Description of the grid

The total drag and lift coefficients are defined, respectively, as:

$$C_{DT}(t) = C_{DFoil} + C_{DRod} = \frac{F_{1X}(t)}{\left(\frac{1}{2}\right)\rho\left(U(t)\right)^2 C\ sin\alpha} + \frac{F_{2X}(t)}{(1/2)\rho(U(t))^2 d}$$

$$C_{LT}(t) = C_{LFoil} + C_{LRod} = \frac{F_{1y}(t)}{\left(\frac{1}{2}\right)\rho\left(U(t)\right)^2 C\, cos\alpha} + \frac{F_{2y}(t)}{(1/2)\rho(U(t))^2 d}$$

where, $F_{1X}(t)$ and $F_{2X}(t)$ represent, respectively, the instantaneous total force in the x-direction (longitudinal) apply in the foil and in the rod, $F_{1y}(t)$ and $F_{2y}(t)$ represent, respectively, the instantaneous total force in the normal(transversal) direction apply in the foil and in the rod, t, the time, c the foil chord, and d the diameter rod.

The instantaneous total force defined as

$$F(t) = F_P(t) + F_S(t)$$

where $F_P(t), F_S(t)$ represent, respectively, the generated pressure force and wall shear force.

A. Mesh Independence

To study the simulation results mesh independent, many cases were simulated with several mesh concentrations. The number of cells used in all cases was between 2 and 3 million. Generally, we require a larger number of cells to realize mesh witch is able to give a good estimation of aerodynamic forces and flow characteristics. The pressure distribution over the foil surface for the natural case (without a rod) was also compared with those given by Serdar Genç [1]. The maximum error was about 3%. The curves plotted in Fig.3 show a good agreement between this study and the previous works.

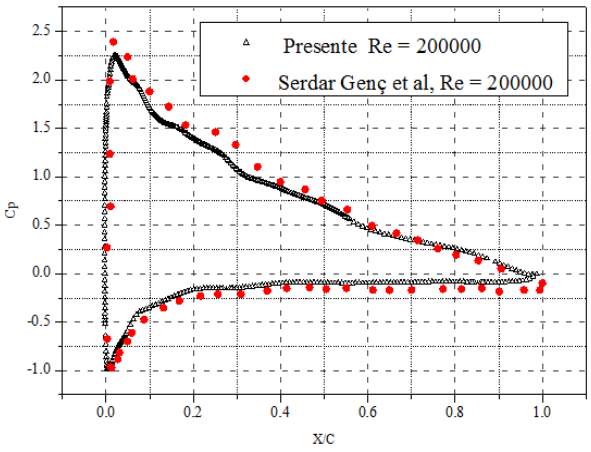

Fig. 3 Pressure coefficient

III. Drag and Lift Coefficients

The time history of lift and drag coefficients indicated in Fig. 4 show that the lift and the drag oscillate in time with a quasi-sinusoidal way. These oscillations are due to the periodic vortex shedding mechanism. As seen in Figs. 5 and 6 there is a decrease in the total lift coefficient and an increase in that of drag due to the weak interaction between the rod wake and the leading edge vortices, also to the formation of small structures which develop along the upper surface (Fig. 10).

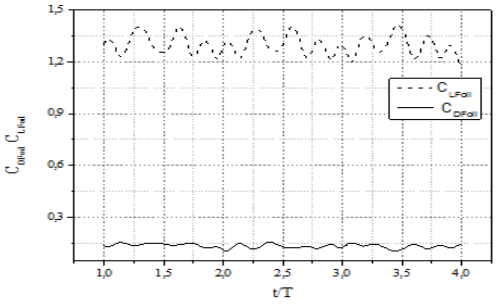

Fig. 4 Time history of lift and drag coefficients

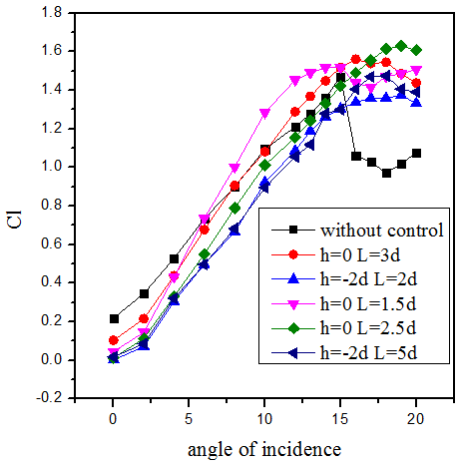

Fig. 5 Time-averaged total lift coefficient

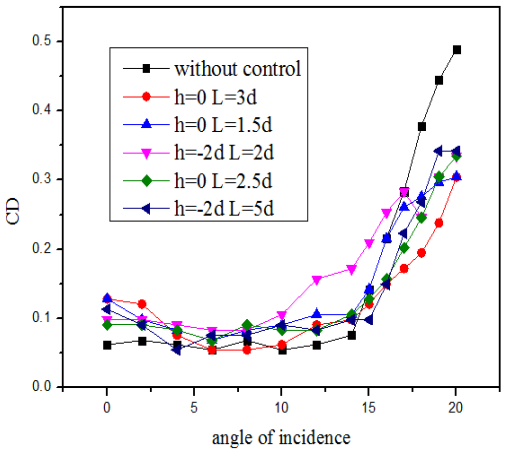

Fig. 6 Time-averaged total drag coefficient

Compared with the controlled cases, the mean pressure coefficient Cp plotted in Fig. 3 indicate that for the case without control an isobar plateau corresponds to the separation bubble appear in the upper surface. The skin friction coefficient Cf, on the upper surface of the airfoil is shown in Fig. 8. The negative value of Cf correspond to the near-wall reversed flow in the separation bubble. The skin friction curve for the case without control indicates that the separation starts at x = 0.05C near the leading edge. The separated flow

reattaches near x = 0.21C. The average length of the separation bubble is about 0.15C. The Cf curves for all cases with control indicate a reducing or a total elimination of the laminar separation bubble.

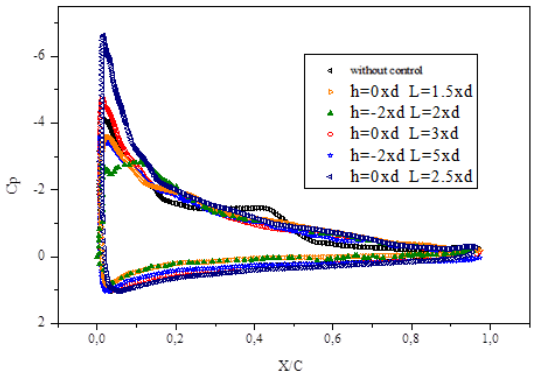

Fig. 7 Mean pressure coefficient

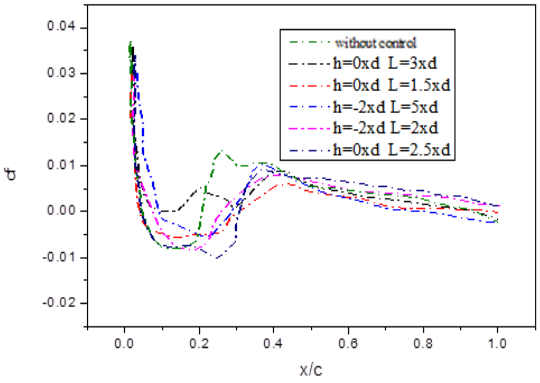

Fig. 8 Mean skin friction coefficient

The mean pressure coefficient curves show an increase in depression at the leading edge results in an increase in the lift coefficient. The best performances for the drag reduction are case $h = 0, L = 3 \times d$ with a value of 50%. In this case, the lift is not the largest this one is marked for the case $h = 0, L = 2.5 \times d$ with a value of 35%.One notes that the location and length of the separation bubble are changed under the control effect.

IV. Flow Visualization

The instantaneous fields of vorticity which show creation, the development and detachment of the flow vortices are given in Figs. 9 and 10. We noted that the zone of recirculation does not exist at the leading edge; in fact, the wake of the rod interacts with the separated zone and formed small structures which developed along the upper surface. We remarked, also, the presence of the Kelvin-Helmholtz waves which occur starting from the trailing edge. These waves are vortices which appear when the velocity profile presents a point of inflection and is characterized by a strong amplification rate. The difference in velocity between the under and the upper surface of the foil induces also a shearing in the mixture layer.

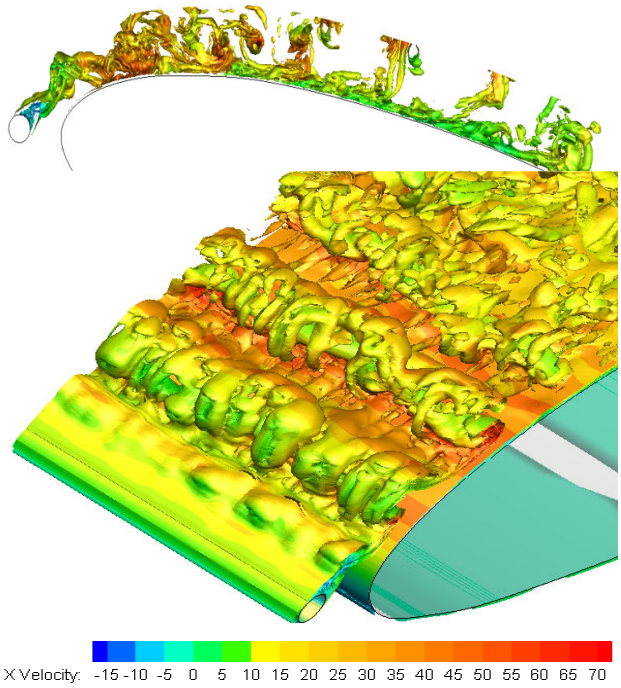

Fig. 9 Iso surface of vorticity colored by the longitudinal velocity case $h = 0, L = 1.5 \times d$

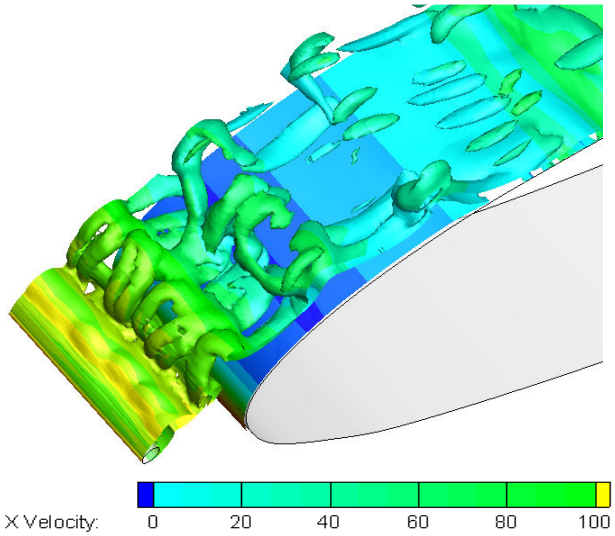

Fig. 10 Iso surface of vorticity colored by the longitudinal velocity case$h = 0, L = 3 \times d$

V. Conclusion

In this study we considered the effect induced by the presence of a rod in the aerodynamics coefficients and flow structure. We noted a total modification in the flow behavior. Our results show that the laminar separation disappears completely in the optimal case and a maximum drag reduction of 50%was registered.

REFERENCES

[1] Serdar Genc, M., Hakan,kAcıkel, H. An experimental study on aerodynamics of NACA2415 aerofoil at low Re numbers Journal of Experimental Thermal and Fluid Science: 10.1016.
[2] Mittal R., Kotapati R.B. et Cattafesta L. 2005. "Numerical study of resonant interactions and flow control in a canonical separated flow". AIAA Paper, No. 2005-1261.
[3] Greenblatt D, Wygnanski IJ. The control of flow separation by periodic excitation. Prog Aerospace Sci 2000;36:487–545.
[4] amotsu Igarashi. (1997) "Drag reduction of a square prism by flow control using a small rod". Journal of Wind Engineering and Industrial Aerodynamics; 69 71 141-153.
[5] Igarashi, T., Nobuaki, T.Drag reduction of flat plate normal to airstream by flow control using a rod .Journal of Wind Engineering and Industrial Aerodynamics 90 (2002) 359–376.
[6] T. Sutsui, Igarashi, T. Drag reduction of a circular cylinder in an air-stream Journal of Wind Engineering and Industrial Aerodynamics 90 (2002) 527–541.